

***Final Draft***  
**of the original manuscript:**

Schmoelzer, T.; Stark, A.; Schwaighofer, E.; Lippmann, T.; Mayer, S.;  
Clemens, H.:

**In Situ Synchrotron Study of B19 Phase Formation in an  
Intermetallic Gamma-TiAl Alloy**

In: Advanced Engineering Materials (2012) Wiley

DOI: 10.1002/adem.201200047

DOI: 10.1002/adem.((please add manuscript number))

## **In-situ synchrotron study of B19 phase formation in an intermetallic $\gamma$ -TiAl alloy\*\***

By *T. Schmoelzer\**, *A. Stark*, *E. Schwaighofer*, *T. Lippmann*, *S. Mayer*, and *H. Clemens*

[\*] *T. Schmoelzer, E. Schwaighofer, Dr. S. Mayer, Prof. Dr. H. Clemens*  
*Department Physical Metallurgy and Materials Testing,*  
*Montanuniversität Leoben, 8700 Leoben, (Austria)*  
*E-mail: thomas.schmoelzer@unileoben.ac.at*  
*Dr. A. Stark, Dr. T. Lippmann*  
*Institute of Materials Research,*  
*Helmholtz-Zentrum Geesthacht, 21502 Geesthacht, (Germany)*

[\*\*] *The support of DESY management, User Office and HZG beamline staff is highly acknowledged. Research activities leading to the presented HEXRD results received funding from the European Community's Seventh Framework Programme (FP7/2007-2013) under grant agreement n°226716. A part of this project was conducted within the framework of the BMBF project O3X3530A, Germany and the Styrian Materials Cluster, Austria.*

*A multitude of phases exists in the binary Ti-Al phase diagram and even greater numbers are formed in structural TiAl alloys, which contain additional alloying elements to improve their properties. In the current study, a Ti-45 Al-3 Mo-0.1 B (in at%) alloy was investigated with respect to the phases occurring in chemical disequilibrium. In-situ high energy X-ray diffraction experiments enabled to identify a transient phase to be of the B19 type and to determine its temperatures of formation and dissolution.*

### Introduction

As there is increasing pressure on manufacturers to produce more efficient and lightweight aircraft engines, new material classes are considered for structural components. Among the prime candidates to replace dense Ni-based super-alloys in the low pressure turbine are materials in the Ti-Al alloy system.<sup>[1]</sup> A range of alloying elements is used to adjust their properties and among them is Mo, a strong stabilizer of the  $\beta/\beta_0$ -phase.<sup>[2, 3]</sup> This phase is of great technological importance due to its beneficial effects on the solidification and hot-deformation behavior of  $\gamma$ -TiAl alloys. For further information on the role of  $\beta/\beta_0$ -phase in  $\gamma$ -TiAl based alloys, the reader is referred to.<sup>[4, 5]</sup>

To improve the understanding of the effects of Mo addition to  $\gamma$ -TiAl based alloys, an alloy with a nominal composition of Ti-45 Al-3 Mo-0.1 B (in at%) was produced. The phases occurring in this alloy were studied by means of in-situ high-energy X-ray diffraction (HEXRD) over a wide temperature range<sup>[6]</sup> and it was attempted to construct a phase diagram from the results of this study and information published in the literature.<sup>[7]</sup> In technological processes, however, high heating and cooling rates are frequently used. Therefore, the materials behavior under disequilibrium conditions is investigated in the current study.

In equilibrium conditions the phases  $\alpha_2$  (D0<sub>19</sub>, P63/mmc),  $\beta_0$  (B2, Pm-3m) and  $\gamma$  (L1<sub>0</sub>, P4/mmm) are present at room temperature. At high temperatures,  $\alpha_2$  and  $\beta_0$  disorder to  $\alpha$  (A3, P63/mmc) and  $\beta$  (A2, Im-3m), respectively. The transformation temperatures are 1205 °C for  $\alpha_2 \rightarrow \alpha$  and ~1230 °C for  $\beta_0 \rightarrow \beta$ .<sup>[8]</sup> Details on the phase diagram can be found in.<sup>[6,7]</sup> In addition to these main constituents, several phases with lower symmetry are mentioned in literature. Among these are hexagonal  $\omega$ -related phases<sup>[9]</sup> and orthorhombic phases.<sup>[10,11]</sup> Abe et al.<sup>[10]</sup> reported on an orthorhombic phase with B19 structure (Pmma) that forms very fine precipitates upon rapid cooling in a Ti-48 Al alloy. Tanimura et al.<sup>[12]</sup> observed the formation of B19-phase as a metastable transitional phase during the A3 $\rightarrow$ D0<sub>19</sub>+L1<sub>0</sub> precipitation sequence. Here also small regions of B19 were formed in the  $\alpha/\alpha_2$  matrix upon quenching of a Ti-40 Al alloy from 1250 °C which acted as nucleation sites for  $\gamma$ -phase formation during a subsequent annealing step at 1000 °C. Appel et al.<sup>[11]</sup> observed B19 phase in Ti-(40-44) Al-8.5 Nb alloys after extrusion at 1250 °C and a subsequent heat-treatment at 1030 °C. Although the existence of the B19 phase in the TiAl system has been well established, no detailed information on the chemical or temperature regime in which the B19 phase form in these alloys is available as yet.

It should be noted that the B19-phase is structurally closely related to the  $\alpha/\alpha_2$ ,  $\gamma$  and  $\beta/\beta_0$  phase.<sup>[13]</sup> Figure 1 a shows a hexagonal closest packed plane in which only atoms of one kind are present which corresponds to the {0001} plane of the disordered  $\alpha$ -Ti(Al) phase. In

**Figures 1 b** and **c** closest packed planes are presented which are composed of two atomic species with compositional ratios of 3:1 or 1:1, similar to the {0001} plane in  $\alpha_2$ -Ti<sub>3</sub>Al and the {100} plane in B19-TiAl, respectively. All three phases exhibit the stacking sequence ...ABAB... which corresponds to that of a hexagonal closest packed structure. Nonetheless possesses the B19 structure an orthorhombic symmetry due to the fact that the two atomic species are arranged in alternating lines (**Figure 1 c**). It should be noted, however, that the B19 lattice is only slightly distorted as compared to an ideal hexagonal lattice.

It is interesting to note that the atoms in the closest packed plane of  $\gamma$ -TiAl (which is the {111} plane) are aligned in the same way as in the {100} plane of the B19 structure (**Figure 1 c**). Contrary to B19, however, the L1<sub>0</sub> structure exhibits the stacking sequence ...ABCABC... Also in  $\beta_0$ -TiAl, the atomic arrangement in the closest packed plane (which is the {110} plane) corresponds to that of the {100} plane of B19 (**Figure 1 c**). The structural relationship between B19 and  $\beta_0$  is similar to that between  $\alpha$  and  $\beta$ -Ti.

### *Experimental*

The phases occurring in disequilibrium in a Ti-44.58 Al-3.23 Mo-0.12 B alloy were investigated by means of in-situ HEXRD experiments at the HARWI II beamline of the DESY synchrotron in Hamburg, Germany.[14] Details on ingot production, phase diagram and original microstructure can be found in.[6, 7] Diffraction experiments were conducted with a beam of monochromatic synchrotron radiation which had a mean energy of 100 keV and a cross-section of 1x1 mm<sup>2</sup>. Heating of the cylindrical specimens with a diameter of 5 mm and a length of 15 mm was performed by a modified Bähr DIL 805A/D dilatometer.[15] Temperature control was achieved by means of an S-type thermocouple. Note that the temperatures given in this paper are rounded to 5 °C steps. A mar555 detector (marresearch, Norderstedt, Germany) recorded the diffraction patterns at a distance of 1837 mm from the specimen position. Integration of the diffraction patterns was performed by

means of the fit2D software package.[16] For Rietveld fitting, the software PowderCell was employed.

Prior to the in-situ experiment, the specimens were heat treated at 1450 °C for 30 min and subsequently water quenched. This resulted in a  $\alpha_2+\beta_0$  microstructure where the  $\alpha_2$ -phase formed rapidly during cooling and is in chemical disequilibrium. Due to the suppression of  $\gamma$ -phase formation, the  $\alpha_2$ -phase is highly supersaturated in Al. Heating during the HEXRD experiments was performed continuously at rates of 25 °C/min and 2 °C/min.

## Results and Discussion

Employing HEXRD allowed monitoring the evolution of the occurring phases in-situ. A number of selected diffractograms recorded during heating at 2 °C/min are presented in **Figure 2**. The first pattern acquired at 565 °C features single peaks of the  $\alpha_2$  and  $\beta_0$ -phase as indexed in Figure 2. At this temperature, the phase fractions as determined by means of Rietveld analysis are approximately 80 vol%  $\alpha_2$  and 20 vol%  $\beta_0$ . As temperature rises, the  $\alpha_2$  peaks with the general indices 20-21 and 22-41 begin to split. This is most obvious for the peaks 20-20 and 22-40 at a temperature of 640 °C where the separation between the original and the newly emerged reflection reaches a maximum. As the temperature is increased further, the peak splitting gradually diminishes until (at 715 °C) a single peak is visible again. Within this temperature interval the intensity of the  $\gamma$ -peaks has also changed significantly. Starting out with low intensities below 640 °C, a gradual gain in intensity with increasing temperature is observed. Simultaneously, the intensity of the  $\alpha_2$  reflections is abating. At a temperature of 715 °C a phase composition of about 35 vol%  $\alpha_2$ , 20 vol%  $\beta_0$ , and 45 vol%  $\gamma$  is attained.

## Figure 2

When heating with a higher rate (25 °C/min), the diffraction patterns show similar changes, but shifted to higher temperatures. The splitting of  $\alpha_2$ -phase reflections starts at about 650 °C and the maximum peak separation is reached at approximately 710 °C. The appearance of the  $\gamma$  reflections and the reduction in  $\alpha_2$ -peak intensity occurs at 740 °C.

In order to investigate if any microstructural changes occurred during heating to 640 °C, one specimen was heated to this temperature (also at a rate of 2 °C/min) and subsequently quenched. This specimen and a second one which was only subjected to the primary heat-treatment at 1450 °C and quenched were prepared for scanning electron microscopic (SEM) investigations by means of standard metallographic methods.<sup>[17]</sup> Comparison of the microstructural images obtained showed that no apparent changes occurred. The microscopical image of the specimen heated to 640 °C is shown in **Figure 3**. It was obtained in back scattered electron (BSE) mode by means of a Zeiss EVO 50 SEM. Only two phases ( $\alpha_2$  and  $\beta_0$ ) can be distinguished which exhibit morphologies that strongly resemble martensitic microstructures observed in commercial Ti alloys (e.g. <sup>[18, 19]</sup>). Although a small  $\gamma$  peak is observed in the diffraction pattern obtained at 640 °C, no indication for  $\gamma$  formation was found in the micrograph. This might be due to the fact, that  $\gamma$  forms ultrafine lamellae during its early stages of precipitation <sup>[20]</sup> which cannot be resolved in the SEM.

### **Figure 3**

From the sequence of events, it is tempting to speculate that a precursor phase forms in supersaturated  $\alpha_2$  and facilitates the precipitation of  $\gamma$ -phase. The splitting of the hexagonal  $\alpha_2$  reflections 20-21 and 22-41 is indicative of an orthorhombic distortion of the lattice. All former  $\alpha_2$  reflections and the newly split double peaks can clearly be attributed to a transient orthorhombic phase with B19 structure (Pmma) as shown in **Figure 2**. At the temperature where the peak separation is most clearly visible (T=640 °C), the lattice parameters of B19

were evaluated to  $a=4.65 \text{ \AA}$ ,  $b=2.93 \text{ \AA}$  and  $c=4.95 \text{ \AA}$ . It was found that all of the  $\alpha_2$  phase had transformed to B19 and phase fractions of approximately 80 vol% B19 and 20 vol%  $\beta_0$  were determined. Although the finding that all of  $\alpha_2$  transforms to B19 before  $\gamma$  precipitation starts is contrasted by the findings of Abe et al. <sup>[10]</sup> and Tanimura et al. <sup>[12]</sup> it should be taken into account that the alloy compositions are quite different in these studies.

Concerning the formation of B19 it should be noted that the splitting of  $\alpha_2$  reflections increases continuously as temperature rises. One example for the development of double peaks is the former 22-40- $\alpha_2$  reflection which gradually splits into two clearly separated peaks, 020-B19 and 013-B19. This indicates that the formation of B19 is associated with diffusional effects and a continuous change in chemical composition occurs. The observation that the formation temperature of B19 strongly depends on the heating rate supports this conclusion.

In this study it was possible to observe the transformation processes in-situ whereas former studies depended on post mortem analyzed samples. It was, however, not possible to identify any changes between the as-quenched and the state after annealing at 640 °C by means of SEM in back scattered electron (BSE) contrast. Since the chemical compositions and the crystal structures of  $\alpha_2$  and B19 are quite similar, it is not far-fetched to assume that the microstructural changes induced by the phase transformation are too subtle to be detected in the SEM. For this reason, TEM investigations are planned for forthcoming studies.

Unfortunately, no information on the stability of the B19 phase within the observed temperature range was obtained. Further experiments are needed to clarify this matter. This study, however, is the first in which the formation of B19 phase in TiAl alloys was observed in-situ. It was found that B19 forms as a transient phase facilitating the precipitation of  $\gamma$  from  $\alpha_2$ . Furthermore, it was possible to determine the temperature range in which the B19 phase occurs in the investigated alloy

## Conclusion

During heating of a heat-treated and quenched Ti-45 Al-3 Mo-0.1 B alloy (nominal composition), an unexpected transitional phase was observed by means of a high-energy X-ray diffraction method. It was determined that the supersaturated  $\alpha_2$  phase transformed via the orthorhombic B19 phase to  $\gamma$  and  $\alpha_2$ . It was determined that the B19 phase formed in the temperature range from 600-700 °C when a heating rate of 2 °C/min is employed. The close structural relationship between  $\alpha_2$ ,  $\gamma$  and B19 facilitates the formation of this phase and is elaborated in this publication. Since industrial processes are frequently conducted at high heating and cooling rates, the observation of B19 phase formation during processes far from thermal equilibrium has also a strong technological relevance.

Received: ((will be filled in by the editorial staff))

Revised: ((will be filled in by the editorial staff))

Published online: ((will be filled in by the editorial staff))

## References

- [1] H. Clemens, W. Smarsly, *Advanced Materials Research* **2011**, 278, 551-556.
- [2] R. Kainuma, Y. Fujita, H. Mitsui, I. Ohnuma, K. Ishida, *Intermetallics* **2000**, 8, 855-867.
- [3] H. Clemens, W. Wallgram, S. Kremmer, V. Güther, A. Otto, A. Bartels, *Advanced Engineering Materials* **2008**, 10, 707-713.
- [4] F.-S. Sun, C.-X. Cao, S.-E. Kim, Y.-T. Lee, M.-G. Yan, *Metallurgical and Materials Transactions A* **2001**, 32, 1573-1589.
- [5] H. Clemens, H.F. Chladil, W. Wallgram, G.A. Zickler, R. Gerling, K.-D. Liss, S. Kremmer, V. Güther, W. Smarsly, *Intermetallics* **2008**, 16, 827-833.
- [6] T. Schmoelzer, S. Mayer, C. Sailer, F. Haupt, V. Güther, P. Staron, K.-D. Liss, H. Clemens, *Advanced Engineering Materials* **2011**, 13, 306-311.
- [7] S. Mayer, C. Sailer, H. Nakashima, T. Schmoelzer, T. Lippmann, P. Staron, K.-D. Liss, H. Clemens, M. Takeyama, *MRS Proceedings* **2011**, 1295, 113-118.
- [8] S. Kabra, K. Yan, S. Mayer, T. Schmoelzer, M. Reid, R. Dippenaar, H. Clemens, K.-D. Liss, *International Journal of Materials Research (formerly Zeitschrift fuer Metallkunde)* **2011**, 102, 697-702.



- [9] A. Stark, M. Oehring, F. Pyczak, A. Schreyer, *Advanced Engineering Materials* **2011**, *13*, 700-704.
- [10] E. Abe, T. Kumagai, M. Nakamura, *Intermetallics* **1996**, *4*, 327-333.
- [11] F. Appel, M. Oehring, J.D.H. Paul, *Advanced Engineering Materials* **2006**, *8*, 371-376.
- [12] M. Tanimura, Y. Inoue, Y. Koyama, *Scripta Materialia* **2001**, *44*, 365-373.
- [13] A. Stark, *Textur- und Gefügeentwicklung bei der thermomechanischen Umformung Nb-reicher  $\gamma$ -TiAl-Basislegierungen*, Shaker Verlag, Aachen **2010**.
- [14] T. Lippmann, L. Lottermoser, F. Beckmann, R.V. Martins, T. Dose, R. Kirchhof, A. Schreyer, in *Hasylab Annual Report*, Hamburg, Germany **2007**, 113.
- [15] P. Staron, T. Fischer, T. Lippmann, A. Stark, S. Daneshpour, D. Schnubel, E. Uhlmann, R. Gerstenberger, B. Camin, W. Reimers, others, *Advanced Engineering Materials* **2011**, *13*, 658-663.
- [16] A.P. Hammersley, S.O. Svensson, M. Hanfland, A.N. Fitch, D. Hausermann, *High Pressure Research* **1996**, *14*, 235-248.
- [17] R. Schnitzer, H.F. Chladil, C. Scheu, H. Clemens, S. Bystrzanowski, A. Bartels, S. Kremmer, *Praktische Metallographie* **2007**, *44*, 430-442.
- [18] H. Matsumoto, H. Yoneda, K. Sato, S. Kurosu, E. Maire, D. Fabregue, T.J. Konno, A. Chiba, *Materials Science and Engineering A* **2011**, *528*, 1512-1520.
- [19] M. Takeyama, S. Kobayashi, *Intermetallics* **2005**, *13*, 993-999.
- [20] L. Cha, H. Clemens, G. Dehm, *International Journal of Materials Research (formerly Zeitschrift Fuer Metallkunde)* **2011**, *102*, 703-708.

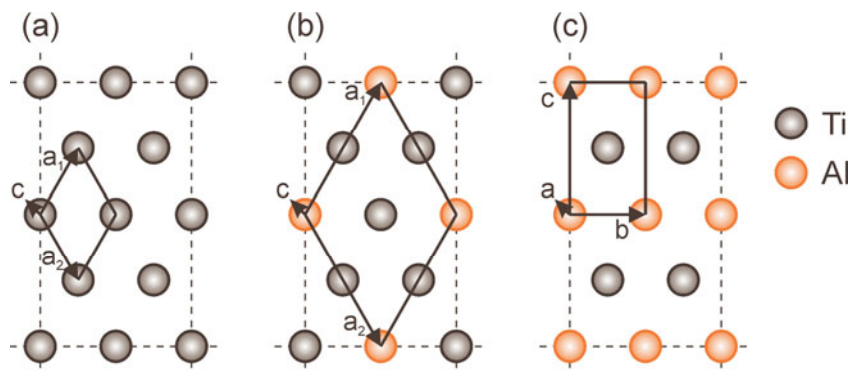


**Figure 1:** Structural relations between the individual phases in TiAl alloys illustrated by sections of their closest packed planes. (a)  $\{0001\}$   $\alpha$ -Ti(Al), (b)  $\{0001\}$   $\alpha_2$ -Ti<sub>3</sub>Al, and (c)  $\{100\}$  B19-TiAl. The dimensions of the unit cells of  $\alpha$ -Ti(Al),  $\alpha_2$ -Ti<sub>3</sub>Al, and B19-TiAl are marked by

solid lines. It should be noted that (a) also corresponds to  $\{110\}$   $\beta$ -Ti(Al) and (c) also corresponds to  $\{111\}$   $\gamma$ -TiAl as well as  $\{110\}$   $\beta_o$ -TiAl.

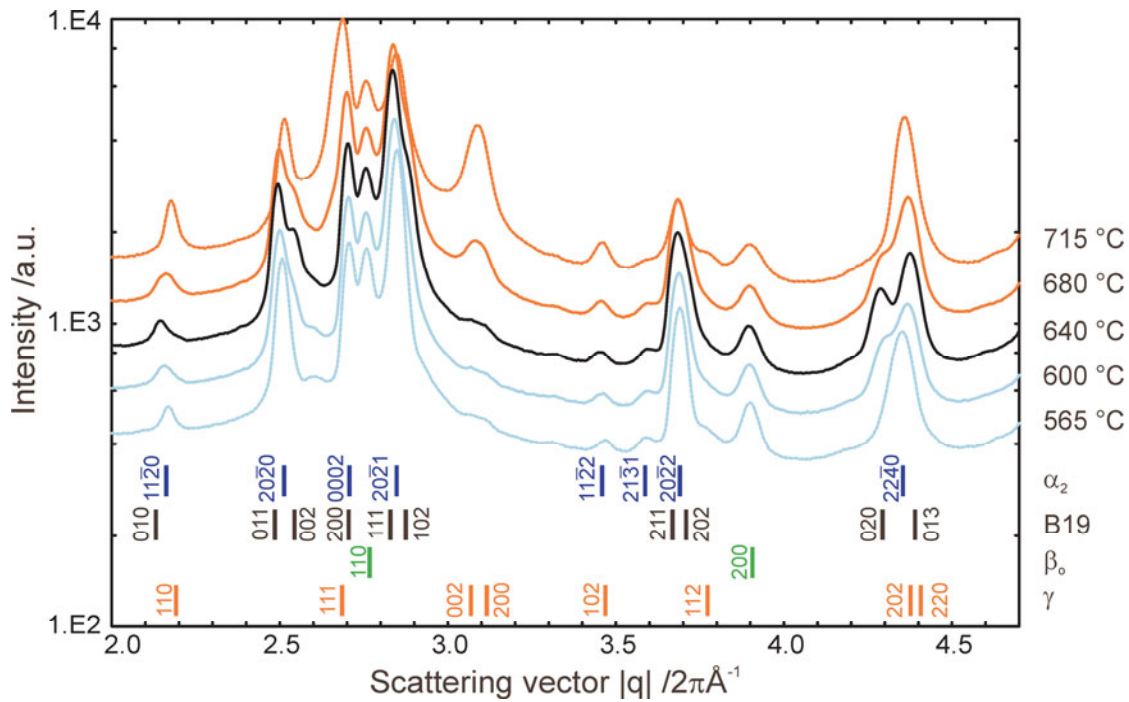


**Figure 2:** Diffractograms obtained by HEXRD during continuous heating. Temperatures at which the patterns were obtained are indicated on the right. It is obvious that peaks of  $\alpha_2$  reflections split due to the formation of the orthorhombic B19 phase. All reflections are indexed at the bottom.

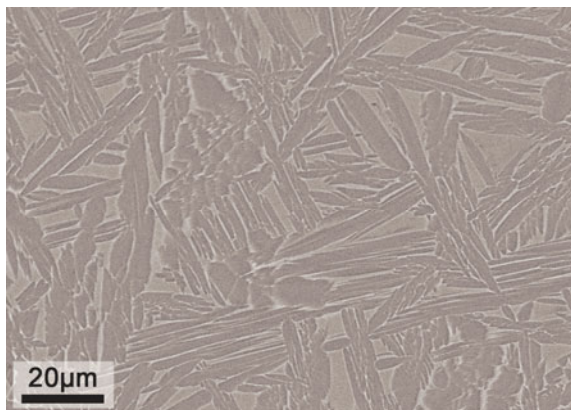


**Figure 3:** SEM micrograph of the specimen after heating to 640 °C at a rate of 2 °C/min. The image was obtained in BSE mode.  $\beta_o$  appears in light grey and B19 in dark grey.

In-situ high-energy X-ray diffraction experiments were conducted on a heat-treated and quenched Ti-45 Al-3 Mo alloy. As shown in the image, B19 phase was formed as a transitional phase during the  $\alpha_2 \rightarrow \gamma$  phase transformation upon heating. In this work, the temperatures of B19 formation and dissolution are given and the structural similarities which facilitate the transformation via a transitional phase are elaborated.

*T. Schmoelzer\*, A. Stark, E. Schwaighofer, T. Lippmann, S. Mayer, and H. Clemens*

In-situ synchrotron study of B19 phase formation in an intermetallic  $\gamma$ -TiAl alloy

